Light Metals 2011 *Edited by: Stephen J. Lindsay*
TMS (The Minerals, Metals & Materials Society), 2011

ADVANCED NUMERICAL SIMULATION OF THE THERMO-ELECTRO-CHEMO-MECHANICAL BEHAVIOUR OF HALL-HÉROULT CELLS UNDER ELECTRICAL PREHEATING

Daniel Marceau[1], Simon Pilote[1,2], Martin Désilets[3], Jean-François Bilodeau[2], Lyès Hacini[2], Yves Caratini[4]

[1]University Research Centre on Aluminium (CURAL) - Aluminium Research Centre (REGAL) - University of Québec at Chicoutimi; 555, Boul. de l'Université, Chicoutimi (Québec), Canada, G7H 2B1
[2]Rio Tinto Alcan (Arvida Research and Development Center), P.O. Box 1250, Jonquière (Québec), Canada, G7S 4K8
[3]Aluminium Research Centre (REGAL) – Sherbrooke University; 2500, Boul. de l'Université; Sherbrooke (Québec), Canada, J1K 2R1
[4]Rio Tinto Alcan (Laboratoire de recherche des fabrications); BP 114, 73303 Saint-Jean-de-Maurienne Cedex - France

Keywords: Hall-Héroult Cell, Electrical Preheating, Energy Consumption, Thermo-Electro-Mechanical Simulation, Finite Element Method

Abstract

In today's context, aluminum producers strive to improve their position regarding energy consumption and production costs. To do so, mathematical modeling offers a good way to study the behavior of the cell during its life. This paper deals with the numerical simulation of the electrical preheating of a Hall-Héroult cell using a quarter model of the cell. The fully coupled thermo-electro-mechanical model includes material non linearities and multiphysical behavior at interfaces allowing accurate evaluation of the stress distribution in the cathode blocks and surrounding components. The baking of the ramming paste as well as the evolution of its thermo-electro-mechanical properties are updated via the baking index computed using a kinetic of reaction. The model is initially calibrated with *in situ* measurements and then used to estimate the effect of preheating on the behavior of the cell including temperature, current, deformations as well as the contact conditions at critical interfaces.

Introduction

The Hall-Héroult process is still and will remain for a long time, the most popular process used to produce aluminum (Al). This high-temperature electrolytic process starts with the dissolution of alumina in a molten cryolite. The electrical voltage used in a typical reduction cell is in the range of 4 to 5 V, but requires high amperage in the range of 150 to 500 kA depending on the technology.

Considering today's available data, the best technology uses approximately 12.5 to 13.0 MW/t of Al which is quite far from the theoretical value of 6.0 MW/t. Applied to the Québec smelters, this actual consumption corresponds to 14% of the installed capacity of Hydro-Québec. A value of 11 MW/t of Al is targeted by the industry before 2020. In the same way, the typical reduction cell has an average lifespan of about 2,500 days which corresponds to approximately 25 kg of spent pot lining per ton of Al. Canadian smelters produce approximately 65 kt of spent pot lining per year. Moreover, considering that the replacement cost of a typical cell is roughly ranging from 100 to 350 k$ CND, an increase of its lifespan is therefore an efficient way to reduce the production cost as well as the middle- to long-term impacts for the environment.

Considering the large number of operating reduction cells in the world, it is natural to investigate the ways to increase the amperage of these cells without any significant negative impacts on its operating cost, lifespan and for the environment. To do this, a solid understanding of the behavior of the cell during its start-up stage as well as during its production stage is a crucial issue.

In particular, recent technological advances have still demonstrated that the lifespan of a reduction cell is strongly conditioned by the start-up stage. However, it remains very difficult to evaluate the quality of a good start-up because of many factors influencing this stage mainly dedicated to ensure smooth transition to the production stage. Figure 1 shows one published opinion that the start-up stage represents 25% of the total influence on its lifespan.

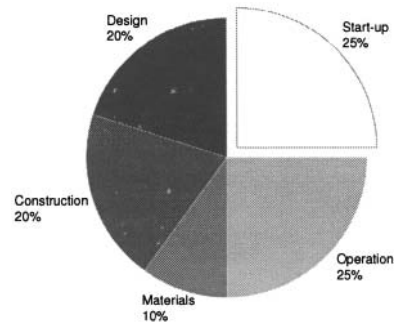

Figure 1 – Relative importance of impact factors on the lifespan of a typical reduction cell [1].

According to [2], a good start-up should include a preheating phase to smoothly increase the temperature in the cell in order to ensure sealing of the cathode plane and avoid thermal shock in the cathode blocks during the bath/molten metal additions. The sealing of the cathode plane is ensured by the ramming paste located between the carbon blocks and between the carbon blocks and the side wall. The quality of the sealing is not only associated to the recipes of ramming paste but also, to the global stiffness of the reduction cell as well as the intensity of the compressive stress distribution developed in the cathode blocks during the preheating stage.

The preheating rate should also be slow enough to avoid a non uniform thermal distribution allowing a large thermal gradient in the cathode blocks. Excessive thermal gradient may result in a loss of stiffness due to crack initiation in the carbon blocks and therefore, in a loss of sealing. On the other hand, a too slow preheating rate may also result in inadequate sealing conditions due to insufficient baking of the ramming paste to produce sufficient compressive stress in the cathode blocks. At the end of the preheating, the temperature in the cathode blocks should be high enough to avoid bath freezing as well as the flash pyrolysis of the ramming paste during bath addition. At this time, the

cathode blocks and the ramming paste should provide a sufficient mechanical resistance to allow the bath/molten metal additions without any damage.

All these concerns show that the investigation of reduction cell under preheating is important but not an easy task. In this paper, the electrical preheating of a P155 reduction cell is investigated using a thermo-chemo-electro-mechanical quarter cell model. The model takes into account the realistic behavior of the most significant components in the cell as well as the interfacial behavior between them. The fully coupled problem is solved using the in-house FE code FESh++ [3] which is one of the most efficient tools to solve this transient highly non linear multiphysical problem.

Previous work

During the last 35 years, several numerical models have been proposed to simulate the behavior of the electrolytic cell or parts of it such as anode assembly, shell, cradles, coke bed, etc. During the first 25 years, most of these models were dedicated to the thermo-electrical behavior of the cell. Despite the large interest of these models, none of them consider the impact of the thermal field distribution on the electrical, mechanical and chemical response of the cell as well as the impact of the mechanical stress distribution on the thermo-electrical equilibrium. Couplet thermo-electro-mechanical modeling of electrolytic cells was first introduced in 2000 by Hiltmann & Meulemann [4], Richard *et al.* [5], and Désilets *et al.* [3]. More recently, Richard *et al.* [6] presented a thermo-chemo-mechanical slice model used to predict the impact of the preheating scenario on the stress distribution in the cathode block and the baking level of the ramming paste. In this last paper, the cathode block, the side block, the castable and the ramming paste were modeled using more realistic constitutive laws that contribute to a more accurate evaluation of the stress distribution in these components during the simulation. In 2010, Dupuis [7] presented three approaches for the mathematical modeling of the deformations inside the potshell of the reduction cell including sodium swelling in the cathode block. However, as underlined by the author, these models neglected the impact of the chemical swelling/shrinkage deformation mechanisms of the ramming paste in the early age of the cell on its stiffness changes as well as that caused by a more realistic mechanical response of the carbon components as used by Richard *et al.* [6].

Physical aspects

Mathematical modeling of the behavior of electrolytic cells during the electrical preheating phase involves complex physical phenomena and their interactions in the continuous media but also at the interfaces between solids. During the electrical preheating, a high amperage electrical current is applied to the cell during a specific time allowing an important increase of the temperature in the components of the cell due to the Joule's law. These temperature changes have an impact on the electrical, thermal and mechanical properties of the cell components including the effect of the baking level of the ramming paste as well as the curing level of the refractory concrete. These complex phenomena (baking, curing) are related to the evolution of a kinetic model assuming a first order reaction rate such as described by the Arrhenius law.

From the mechanical point of view, all these changes allow various strain mechanisms which play a major role in the conditioning of the cell before the molten bath and metal additions. With the exception of the classical thermal expansion and elastic strain which take place within the cell during the preheating, other mechanisms such as plastic strain of the carbon-like components and chemical swelling/shrinkage of the ramming paste should be considered. Over this preheating phase, other mechanisms such creep of steel and cast iron components as well as the sodium swelling of the cathode block should be considered but are not treated in this paper.

At the interfaces, all these changes may have an impact on the electrical and thermal contact resistances which are function of the temperature and the mechanical pressure [5]. Some of these interfaces are critical regarding the energy consumption of the cell such as the cast iron to carbon interfaces where an initial gap distribution takes place before the start-up. Considering the possibility of failure in the carbon block, the contact forces at these interfaces should be computed using the appropriate frictional coefficient. Indeed, the difference of thermal expansion coefficient for the cast iron and the carbon allows moderate relative sliding between both components. If sliding is not allowed, the resulting contact force (normal and frictional) may induce failure in the carbon block. Also, the evolution of the thermo-mechanical contact condition between the shell and the cradle must be considered to allow possible separation. Otherwise, the global stiffness of these components will be overestimated leading to an unrealistic stress state in the components of the cell.

The solution of such a problem is obtained by solving a transient coupled non linear system of equations representing the global thermo-electro-chemo-mechanical equilibrium at anytime.

Finite element model

The finite element model presented in this paper is based on the P155 technology such as that used at Usine Grande-Baie in Saguenay (Québec). This cell consists of 24 anodes and 16 cathode blocks and operates at approximately 185 kA. The model is built using ANSYS® version 11.0 and solved using the finite element toolbox FESh++ which is widely used for the solution of complex multiphysical problems.

Description of the geometrical model

Figures 2 to 4 show a step-by-step construction of the P155 quarter cell model. More specifically, Figure 2 shows the shell/cradle assembly. The shell is supported by the cradles via thermo mechanical contact at the interfaces, and the cradles are simply supported by the concrete beam located below the cradles via mechanical contact. Regarding the components inside the cell, Figure 3 shows the side wall and pier components as well as the carbon blocks and the ramming paste. The side wall is connected to the shell, pier and ramming paste via thermo-mechanical contact. Also, the cathode blocks are linked to the ramming paste using a thermo-mechanical contact considering that the ramming paste is not a good electrical conductor during the first hours of baking. The link between the small joint and the big joint is ensured via thermo-mechanical contact to avoid excessive tensile stress during the preheating. At the cast iron to carbon interface, a thermo-electro-mechanical contact law is used with an initial air gap distribution and the interface between cast iron, the collector bar being assumed perfectly linked. It should be noted that the end and corner walls are not included in the model in order to decrease the number of mechanical DOFs. These components are replaced by equivalent thermo-mechanical contact properties using the thermal conductivity, the Young's modulus and the

thickness of each component. Also, it is assumed that the components below the cathode blocks do not contribute to the bending stiffness of the cathode assembly. In this way, the components are replaced by equivalent mechanical stiffness and thermal conductivity using the approach described above. As shown on Figure 3, a virtual support is used to ensure the mechanical stability of the cathode blocks, the side wall and the pier. To avoid an increasing of the shell stiffness, this virtual support is linked to the shell floor but in contact with the inclined wall of the shell.

Figure 4 shows the full model including the anode assembles which are connected to a virtual anode beam mainly used to apply the current into the cell allowing a more realistic current distribution in each anode. A thermo-electrical contact interface is used to simulate the coke bed using thermo-electrical contact resistance based on the work of Laberge *et al.* [10]. Finally, the flexibles are perfectly connected to the collector bars as well as to the busbars which are thermo-electrical components.

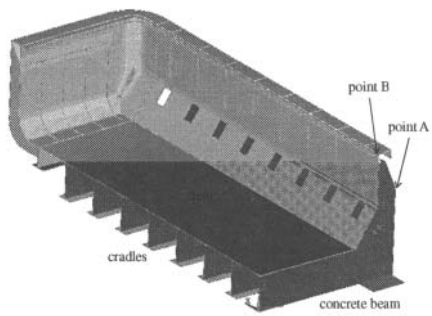

Figure 2 – P155 quarter cell geometry: shell and cradles.

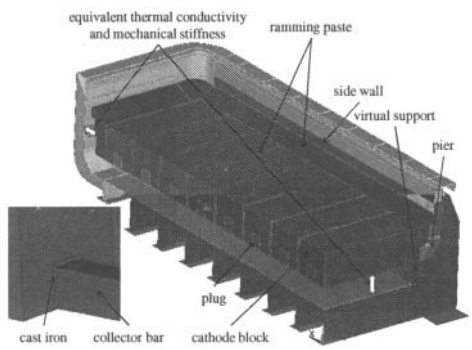

Figure 3 – P155 quarter cell geometry: side wall, pier, ramming paste, cathode blocks, collector bars, cast iron and plug.

Material properties

As described previously, the good representation of the confinement level in the cell during the preheating involves the utilization of realistic constitutive laws. To do so, the carbon-based materials such as cathode block and the ramming paste are modeled using the quasi-brittle with softening constitutive law developed by D'Amours *et al.* [8]. To adequately describe the evolution of the thermal and mechanical parameters during baking of the ramming paste, the above-mentioned law is coupled with a kinetic model described by first order reaction rate as proposed by Richard *et al.* [9]. Considering the large stiffness of components located in the side wall and the pier, their corresponding materials are considered thermo-elastic during the preheating.

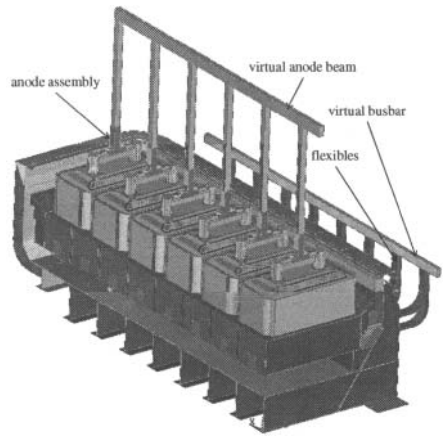

Figure 4 – P155 quarter cell geometry: anode assembly, anode beam, flexible and busbar.

Regarding the contact interfaces, the thermo-electrical contact resistance used for the coke bed is such as described by Laberge *et al.* [10]. A pressure dependant thermo-electrical contact resistance is defined using the approach proposed by Richard *et al.* [5] at the cast iron to carbon interface. For mechanical interfaces where frictional contact occurs, a frictional coefficient should be used. Considering the contact interfaces with carbon-based materials, the frictional coefficient is set to 0.08 which represents a moderately lubricated interface.

Most of the material properties used in this model are confidential and therefore, cannot be published in this paper.

Boundary conditions

The essential electrical boundary condition consists of a zero voltage applied at the exit of the busbars. The essential mechanical boundary conditions are mainly those needed to describe the double symmetry of the quarter cell model. Also, the three displacements on the surface of the concrete beam are prescribed.

Regarding the natural electrical boundary conditions, amperage of 185kA/4 is applied to the quarter cell on a small area located at mid-length on the virtual anode beam. For the thermal part, equivalent natural convection/radiation is applied on external surfaces of the shell and cradles using appropriate coefficients. Inside the cell, the presence of crushed bath around the anode blocks is modeled using a small natural convection coefficient on the sides of the anodes and side wall as well as on the surface of the ramming paste. Considering that the tops of the anodes are insulated with mineral wool, natural convection is also applied on these surfaces using appropriate coefficients. The mechanical part consists of the effect of the weight of the anode assemblies on the cathode plane which is modeled using uniform pressure applied on the total surface of the cathode plane.

To ensure the mechanical stability of the numerical model during the first time steps, the mass of each component (except the anode assemblies) is included as a body load. Otherwise, it remains very

difficult to stabilize the contact conditions on the unloaded mechanical system.

Mesh

The mesh presented on Figure 5 is obtained after some mesh refinements required to obtain a converged solution in the regions of elevated electrical, thermal and mechanical gradients. The global mesh includes 350080 elements distributed as shown on Table 1 regarding the type and physic of the elements. Considering the number of degrees of freedom (DOFs) per node, the thermo-electric and mechanical sub-problems include 464855 and 595595 DOFs respectively.

Table 1 – Number of elements for each part of the model

Type	Physic						Total
	E	T	M	TE	TM	TEM	
Solid	-	1248	1776	60776	37794	106000	207594
Shell	-	-	-	-	8358	-	8358
Contact	-	5032	3867	7692	51218	24000	91809
BC	68	38751	3500	-	-	-	42319
Total:	68	45031	9143	68468	97370	130000	350080

E: electrical, T: thermal, M: mechanical, TE: thermo-electrical, TM: thermo-mechanical, TEM: thermo-electro-mechanical, BC: boundary condition.

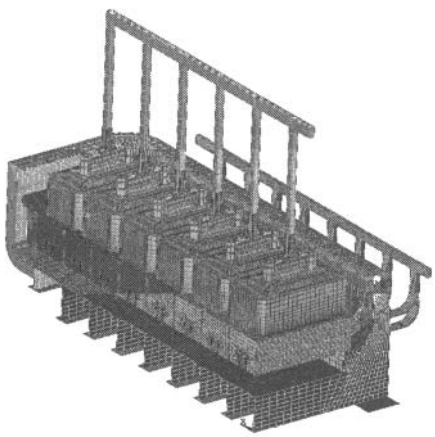

Figure 5 – Mesh of the P155 quarter cell model.

Solution technique

Such kind of problem can be solved using different approaches based on the coupling level. A basic approach is to initially solve the thermo-electrical sub-problem for all the preheating phase without any adjustment regarding the possible effect of the mechanical conditions on the thermo-electrical equilibrium. Later, the mechanical sub-problem is solved for each time step considering the corresponding temperature and voltage distribution for each specific time. Unfortunately, this simple approach cannot be retained in our context considering that the thermo-electrical contact resistance is pressure dependant.

The second approach, which could be designated as the fixed point method, is to solve for each time step the thermo-electrical sub-problem using the last mechanical conditions followed by the solution of the mechanical sub-problem using the last temperature and voltage distributions. Considering that both sub-problems include non-linearities, each of them should be solved using a Newton-Raphson solution technique until convergence. The global convergence is reached when the correction of each field is less than a specified tolerance.

The third approach is to solve the fully coupled non linear problem at each time step using the Newton-Raphson solution technique until convergence. The advantage of this approach is that the linearized system of equations gives a correction for each field simultaneously. This approach allows generally a faster convergence, especially during highly non linear sequences. However, the memory requirement to allow the factorization phase is bigger than that required to solve both sub-problems separately since new couplings appear in the linearized system.

For the time stepping aspect, the problem is solved using a backward Euler time integration scheme with an initial time step of one hour. An adaptive time stepping algorithm is used with a maximum time step of three hours. A bisection technique is used to avoid divergence of the Newton-Raphson solution technique during highly non linear sequences.

The problem is solved using 20 dual core Opteron™ 64 bits compute nodes with 2 Go of RAM per compute node.

As a simple demonstration of the second and third approaches, the Figure 6 shows the CPU time required to solve each time step of a typical preheating of 24 hours using the fully coupled method and the fixed point method. The speed-up of the fully coupled method is a consequence of a better rate of convergence coupled with the adaptive time stepping algorithm. More specifically, the overall CPU time needed to solve this problem by the fully coupled method is 13 hours compared to 24 hours for the fixed point method. The additional memory needed for the factorization of the global problem is simply spread over the 20 cluster nodes used for the simulation.

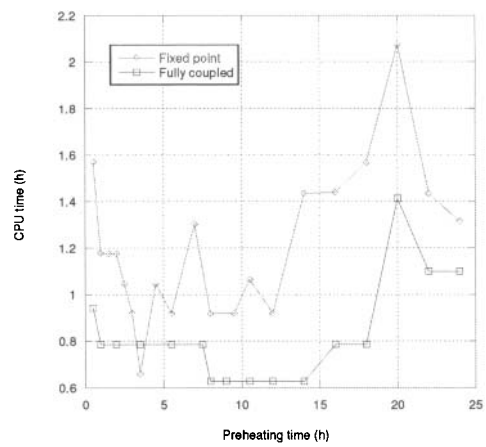

Figure 6 – Fixed point -vs- fully coupled method: Comparison of the CPU time.

Results and Discussion

Sensitivity at the contact interfaces

Before any serious numerical study, the model should be validated regarding the ability of the non physical parameters to give a unique solution. Regarding our problem, the penalty numbers used in the mechanical unilateral contact law are such parameters that need to be calibrated. To do so, six contact interfaces are

investigated. These interfaces are those perpendiculars to or in the vicinity of the critical path where forces go from the cathodes to the shell. Table 2 shows the interfaces under investigation and the four cases which define the combination of penalty number.

Table 2 – Contact interfaces used for the convergence test

Case	Contact interface					
	1	2	3	4	5	6
	Penalty number (N/m^3)					
A	10^8	10^8	10^8	10^8	10^8	10^8
B	10^9	10^9	10^9	10^9	10^9	10^9
C	10^{10}	10^{10}	10^{10}	10^{10}	10^{10}	10^{10}
D	10^{10}	$5{\cdot}10^9$	$5{\cdot}10^9$	10^{10}	10^{10}	$5{\cdot}10^9$

1 – virtual support to sidewall/cathode
2 – cathode to ramming paste
3 – small joint to big joint
4 – cathode to pier
5 – sidewall to shell
6 – sidewall to paste

The case A consists in the first intuitive choice of penalty number which was generally determined by considering the stiffness of the components close to the interface.

The results are obtained for a short preheating of 10 hours. As shown on Figure 2, the horizontal (Z) displacement of point A is monitored for each case. Figure 7 shows that the displacement seems to be converged for the case C or D. However, the case C is a good compromise between speed and accuracy since the computation time generally increases with an increase of the penalty number.

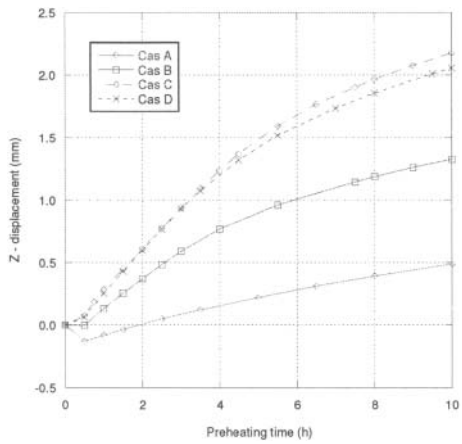

Figure 7 – Effect of the penalty number on the horizontal displacement of point A.

Comparison with *in situ* measurements

Some results are now compared with *in situ* measurements obtained on a P155 electrolytic cell. Considering a preheating of 24 hours, Figure 8 shows the heat-up of three points located on the external face of the shell. At the end of the preheating, the computed temperatures are consistent with those measured with the thermocouples. Considering the electrical results, the average voltage drop between the clads and the end of the collector bars is computed using numerical voltage and compared with the *in situ* average voltage drop. Figure 9 shows that the model can adequately predict the early voltage drop in the cell without any fudging factors to control the total resistivity of the cell. Finally, the horizontal displacement of the deck plate at point B (see Figure 2) during the preheating is shown on Figure 10. The *in situ* measurement is obtained using a survey device. Considering the accuracy of this device, the numerical result extracted at 18 hours is in that range which is ±1mm.

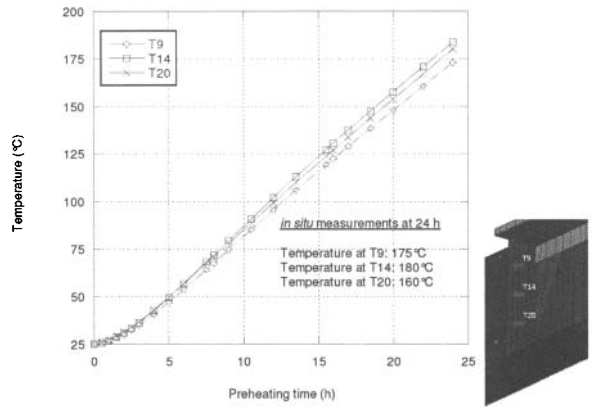

Figure 8 – Comparison with *in situ* results: temperature at three positions on the shell.

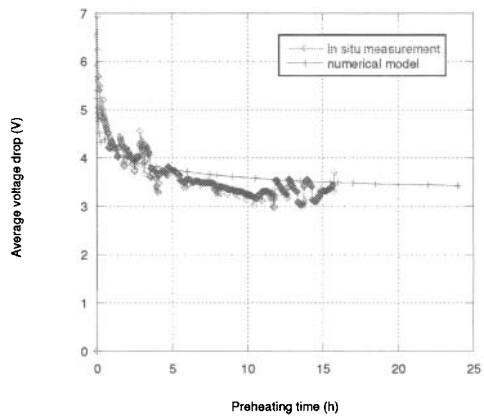

Figure 9 – Comparison with *in situ* results: average voltage drop.

Impact of contact loss

To demonstrate the ability of the model to evaluate the thermo-electro-mechanical contact condition, Figure 11 presents the contact status at the cast iron to carbon interface for each cathode block after 24 hours of preheating. These contact conditions show that sliding and separation occurs in the last four cathode blocks and become more significant for the last cathode blocks. This situation may be explained by the lack of confinement of these cathode blocks combined with the lower temperature in this region of the cell. This separation and/or decrease of contact pressure will adversely affect the current distribution which will be partially redirected to the cathodes located in the center of the cell increasing the current density, and hence, the temperature of these cathode blocks. This situation can be fixed by increasing the stiffness of the shell in this region and by improving the insulation of the end walls which are less exposed to high temperature.

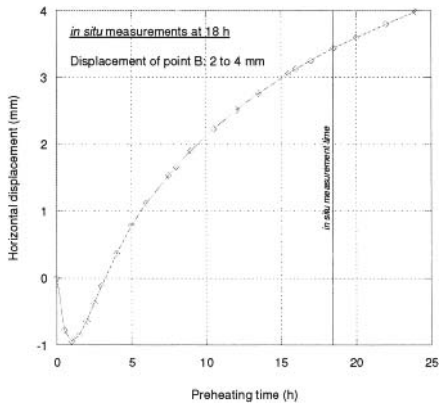

Figure 10 – Comparison with *in situ* results: horizontal displacement of the deck plate (point B).

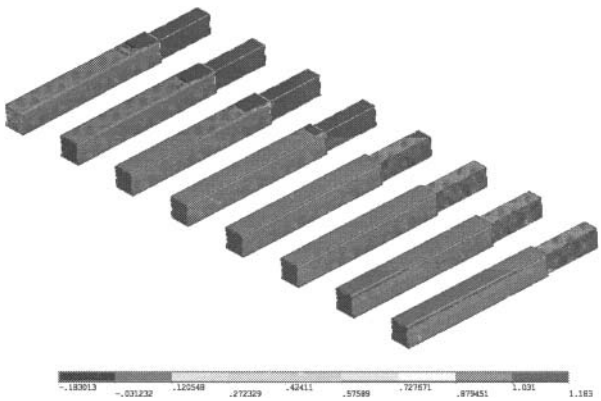

Figure 11 – Contact status at the cast iron to carbon interface (0: non contact, 1: stick contact, 2: sliding contact).

Conclusion

Important works made over the past 10 years have resulted in the development of efficient numerical tools and solution techniques for the simulation of complex multiphysical problems. Combined with the high performance computing facilities, it is now possible to solve very large complex industrial problems in just a few hours. This paper deals with the development of a quarter cell model for the prediction of the thermo-electro-mechanical behavior of Hall-Héroult cell under electrical preheating. More specifically, this P155 model takes into account the quasi-brittle with softening behavior of the carbon-based materials, the change of thermo-mechanical properties of the ramming paste with the baking index as well as the presence of the most critical contact interfaces.

It was demonstrated that the use of a fully coupled solution technique could drastically decrease the computation time. The model has been validated against temperatures, voltages and displacements obtained from *in situ* measurements at Usine Grande-Baie in Saguenay. Finally, the model has been used to evaluate the contact conditions at the cast iron to carbon interfaces in the carbon blocks after a preheating of 24 hours. It shows that the confinement of the last cathode blocks and the insulation of the end wall should be revised.

To ensure a better understanding of the cell over the preheating phase, the actual works are dedicated to the identification of performance indicators for the cell start-up including the bath/metal addition period. To do so, the development of phase change of molten bath, the strain mechanism associated with the sodium migration as well as the creep of cast iron and steel are in progress.

Acknowledgements

The authors would like to thank Dr Guillaume D'Amours from the Aluminum Technology Center for his guidance regarding the thermo-mechanical behavior of the ramming paste and Dr Patrice Goulet from Laval University for his help during the first debugging stage of the quarter cell model. Finally, we thank the Natural Sciences and Engineering Research Council of Canada for its financial contribution via the Industrial Postgraduate Scholarships Program.

References

[1] W.R. Hale, "Improving the useful life of aluminum industry cathodes", *JOM*, 11 (1989), 20-25.

[2] C. Zangiacomi, V. Pandolfelli, L. Paulino, S.J. Lindsay & H. Kvande, "*Preheating study of smelting cells*", TMS Light Metals, 2005, pages 333-336.

[3] M. Désilets, D. Marceau & M. Fafard, "*START-CUVE: Thermo-electro-mechanical transient simulation applied to electrical preheating of a Hall-Héroult cell*", TMS Light Metals, 2003, pages 247-254.

[4] F. Hiltmann, K.H. Meulemann, "*Ramming paste properties and cell performance*", TMS Light Metals, 2000, pages 405-411.

[5] D. Richard., M. Fafard, R. Lacroix, P. Cléry, & Y. Maltais, "*Thermo-electro-mechanical modeling of the contact between steel and carbon cylinders using the finite element method*". TMS Light Metals, 2000, pages 523-528.

[6] D. Richard, P. Goulet, M. Dupuis & M. Fafard, "*Thermo-chemo-mechanical modeling of a Hall-Héroult cell thermal bake-out*", TMS Light Metals, 2006, pages 669-672.

[7] M. Dupuis, "*Using Mathematical modeling of aluminium reduction cell potshell deformation*", TMS Light Metals, 2010, page 417-422.

[8] G. D'Amours, M. Fafard, A. Gakwaya & A. Mirchi, "*Multi-Axial Mechanical Behavior of the Carbon Cathode: Understanding, Modeling and Identification*", TMS Light Metals, 2003, page 633-639.

[9] D. Richard, G. D'Amours, M. Fafard, A. Gakwaya & M. Désilets, "*Development and validation of a thermo-chemo-mechanical model of the baking of ramming paste*", TMS Light Metals, 2005, page 733-738.

[10] C. Laberge, L. Kiss & M. Désilets, "*The influence of the thermo-electrical characteristics of the coke bed on the preheating of an aluminum reduction cell*", TMS Light Metals, 2004, page 207-211.